



U.S. DEPARTMENT OF
ENERGY

PNNL-22424

Boron-10 ABUNCL Prototype Models And Initial Active Testing

Richard T. Kouzes
James H. Ely
Azaree T. Lintereur
Edward R. Siciliano

April 2013



Pacific Northwest
NATIONAL LABORATORY

*Proudly Operated by **Battelle** Since 1965*

DISCLAIMER

This report was prepared as an account of work sponsored by an agency of the United States Government. Neither the United States Government nor any agency thereof, nor Battelle Memorial Institute, nor any of their employees, makes **any warranty, express or implied, or assumes any legal liability or responsibility for the accuracy, completeness, or usefulness of any information, apparatus, product, or process disclosed, or represents that its use would not infringe privately owned rights.** Reference herein to any specific commercial product, process, or service by trade name, trademark, manufacturer, or otherwise does not necessarily constitute or imply its endorsement, recommendation, or favoring by the United States Government or any agency thereof, or Battelle Memorial Institute. The views and opinions of authors expressed herein do not necessarily state or reflect those of the United States Government or any agency thereof.

PACIFIC NORTHWEST NATIONAL LABORATORY

operated by

BATTELLE

for the

UNITED STATES DEPARTMENT OF ENERGY

under Contract DE-AC05-76RL01830

Printed in the United States of America

**Available to DOE and DOE contractors from the
Office of Scientific and Technical Information,
P.O. Box 62, Oak Ridge, TN 37831-0062;**

ph: (865) 576-8401

fax: (865) 576-5728

email: reports@adonis.osti.gov

**Available to the public from the National Technical Information Service,
U.S. Department of Commerce, 5285 Port Royal Rd., Springfield, VA 22161**

ph: (800) 553-6847

fax: (703) 605-6900

email: orders@ntis.fedworld.gov

online ordering: <http://www.ntis.gov/ordering.htm>

Boron-10 ABUNCL Prototype Models And Initial Active Testing

Richard T. Kouzes
James H. Ely
Azaree T. Lintereur
Edward R. Siciliano

April 2013

Pacific Northwest National Laboratory
Richland, Washington 99352

Executive Summary

The Department of Energy Office of Nuclear Safeguards and Security (NA-241) is supporting the project *Coincidence Counting With Boron-Based Alternative Neutron Detection Technology* at Pacific Northwest National Laboratory (PNNL) for the development of a ^3He proportional counter alternative neutron coincidence counter. The goal of this project is to design, build and demonstrate a system based upon ^{10}B -lined proportional tubes in a configuration typical for ^3He -based coincidence counter applications.

This report provides results from MCNPX model simulations and initial testing of the active mode variation of the Alternative Boron-Based Uranium Neutron Coincidence Collar (ABUNCL) design built by General Electric Reuter-Stokes. Initial experimental testing of the as-delivered passive ABUNCL was previously reported.

The efficiency of the reconfigured *active* ABUNCL determined from measurement of a centered ^{252}Cf source was found to be 9.4(5)%, with a die-away time of 83(3) μs . This is compared to the value measured for the *passive* ABUNCL of 11.6(3)%, with a die-away time of 75.2 μs . Combining the efficiency and die-away time gives a FOM (ϵ^2/τ) of 1.1 for the active ABUNCL, compared to a FOM for the passive ABUNCL of 1.8.

The MCNPX model results of the passive configuration provided by GE Reuter-Stokes were reasonably consistent with the results reported [McKinny 2012].

Acronyms and Abbreviations

ABUNCL	Alternative Boron-Based Uranium Neutron Coincidence Collar
AmLi	Americium-lithium neutron source
BWR	Boiling water reactor
cps	Counts per second
DOE	U.S. Department of Energy
ϵ	Detection efficiency
FOM	Figure of Merit
GE	General Electric
GERS	General Electric Reuter-Stokes
HDPE	High Density Polyethylene
IAEA	International Atomic Energy Agency
LEC	Low-Energy Cutoff
MCA	Multi-Channel Analyzer
MOX	Mixed Oxide fuel
NIM	Nuclear Instrumentation Module
NIST	National Institute of Science and Technology
PHL	Pulse-Height Light
PNNL	Pacific Northwest National Laboratory
Pu	Plutonium
τ	Die-away time
TTL	Transistor-transistor logic
U	Uranium
UNCL	Uranium Neutron Coincidence Collar

Contents

Executive Summary	iv
Acronyms and Abbreviations.....	v
Contents	vi
Figures and Tables	vii
1. Introduction.....	1
2. ¹⁰ B-lined ABUNCL Design.....	2
3. ¹⁰ B-lined ABUNCL Active Configuration Testing	4
Efficiency Measurement.....	4
Die-Away Time Measurements.....	5
Repeat of Die-Away Time Measurements	7
AmLi Measurements	10
4. ¹⁰ B-lined ABUNCL Modeling Results.....	11
5. Conclusions.....	24
6. Acknowledgements.....	25
7. References.....	26

Figures and Tables

Figures

Figure 2.1. GE Reuter Stokes ABUNCL at PNNL.....	2
Figure 3.1. GE Reuter Stokes ABUNCL with HDPE Block to Replace Side #2.....	4
Figure 3.2. Doubles rate versus gate width fit for ABUNCL die-away-time.	6
Figure 3.3. Doubles rate versus pre-delay fit for die-away-time.	7
Figure 3.4. Doubles rate versus gate width fit for die-away-time.....	9
Figure 3.5. Doubles rate versus pre-delay fit for die-away-time.	9
Figure 4.1. Side (left) and top (right) cross-sectional views of the B10PNCC model from GERS.....	13
Figure 4.2. Die-away time analyses for the B10PNCC model.	14
Figure 4.3. Pulse-height spectra for individual reaction products and total.	15
Figure 4.4. Comparison of GERS Drawing and GEUNCL upgrade to B10PNCC configuration.	17
Figure 4.5. Left side is side cross-sectional view showing positions for the vertical source profile calculations. Right side is top cross-sectional view through center of active GEUNCL model.....	18
Figure 4.6. Side (left) and top (right) cross sectional views of active GEUNCL model.	18
Figure 4.7. Lethargy plots of energy spectra of several neutron sources. AmLi data are from [Geiger 1971] and ²⁵² Cf data are from [ISO 1989]......	21
Figure 4.8. Energy (top) and source position (bottom) profiles for the passive GEUNCL-P model.	22
Figure 4.9. Energy (top) and source position profiles for the active GEUNCL-A model.	23

Tables

Table 2.1. Characteristics of the UNCL and ABUNCL configurations.	3
Table 3.1. Gate variation data for active configuration die-away time measurement.	5
Table 3.2. Pre-delay data for active configuration die-away time measurement.....	6
Table 3.3. Data for active configuration die-away time measurement.	8
Table 4.1. Results for simplified B10PNCC model compared to PNNL revised version GEUNCL-P.	12
Table 4.2. Effects of changes in boron lining materials and thickness in GEUNCL-P model.....	19
Table 4.3. Results for PNNL Active version, GEUNCL-A.....	19
Table 4.4. Effects of changes in Boron Lining Materials & Thickness in GEUNCL-A model.	20

1. Introduction

The search for technological alternatives to ^3He is a major research area in nuclear security and safeguards due to the shortage of this gas in recent years [Kouzes 2010; Menlove 2011]. One of the important safeguards applications of ^3He has been for coincidence counting instruments. Coincidence counting is a high-precision technique used to measure the mass of plutonium (Pu) or uranium (U) in samples [PANDA 1991]. There are different counter configurations used for different measurement applications. For example, the Uranium Neutron Coincidence Collar (UNCL) and the updated version, the UNCL-II, are used by the International Atomic Energy Agency (IAEA) for verification of the mass of ^{235}U in low-enriched U fuel assemblies [Menlove 1981; Menlove 1990].

The Department of Energy Office of Nuclear Safeguards and Security (NA-241) is supporting the project *Coincidence Counting With Boron-Based Alternative Neutron Detection Technology* at Pacific Northwest National Laboratory (PNNL) for the development of a ^3He proportional counter alternative neutron coincidence counter. The goal of this project is to design, build and demonstrate a system based upon ^{10}B -lined proportional tubes in a configuration typical for ^3He -based coincidence counter applications. Under this project, PNNL has delivered a number of reports on coincidence counting, including an overview [Kouzes 2012a], model validation [Lintereur 2012; Rogers 2012a], wall effect models [Siciliano 2012a], and models of ^3He -based UNCL systems [Siciliano 2012b]. A modeling study of the Alternative Boron-Based Uranium Neutron Coincidence Collar (ABUNCL) determined design parameters for a boron-based alternative to the UNCL [Rogers 2012b].

General Electric (GE) Reuter-Stokes (Twinsburg, OH) has developed a coincidence collar based on arrays of ^{10}B -lined tubes that has been loaned to PNNL for testing against the safeguards requirements for an ABUNCL. The GE Reuter Stokes ABUNCL as delivered was configured as a passive UNCL design for making measurements of fresh Pu-based [mixed oxide (MOX)] fuel.

Monte Carlo modeling of the ABUNCL was performed by PNNL to show agreement with the modeling results reported by GE Reuter-Stokes [McKinny 2012], as well as to compare to the PNNL testing of that design and the PNNL modified active ABUNCL configuration. Following testing of the passive configuration, as reported in [Kouzes 2012b], the system was reconfigured for use in active mode and testing was performed. This paper reports on the results of these two activities.

2. ^{10}B -lined ABUNCL Design

The GE Reuter-Stokes ABUNCL design derives from a cooperative effort between GE Reuter-Stokes and Canberra Industries, Inc. (Meriden, CN) and is based on the Canberra JCC-71 models [Canberra 2011].

The GE Reuter-Stokes ABUNCL assembly consists of 72 boron-lined tubes held in four high-density polyethylene (HDPE) slabs joined together in a rectangular configuration as shown in Figure 2.1. The configuration is such that individual slabs can be removed from the assembly. The assembly has external dimensions of 35 cm x 49 cm x 81 cm, cavity dimensions of 16.5 cm x 23.4 cm, and a total mass of 77 kg. The ten preamplifiers (PDT10A/20A) used in the ABUNCL are manufactured by Precision Data Technology, Inc. (Everett, WA).



Figure 2.1. GE Reuter Stokes ABUNCL at PNNL.

The ABUNCL, as delivered by GE Reuter-Stokes, was configured in a passive boiling water reactor (BWR) coincidence collar configuration.

Table 2.1 shows a comparison of the ^3He based passive BWR UNCL-I and BWR UNCL-II to the results for the GE Reuter-Stokes ABUNCL as reported in [Kouzes 2012b]. The GE Reuter-Stokes design was targeting the UNCL-I performance.

Table 2.1. Characteristics of the UNCL and ABUNCL configurations.

Detector	Total # Tubes, Configuration, & Fuel Cavity H x L x W (cm)	Total No. Moles	Efficiency (ϵ), Die-Away Time (τ) & FOM = ϵ^2/τ					
			Measurement Results			Model Results ¹		
			ϵ	τ (μs)	FOM ($\%^2/\mu\text{s}$)	ϵ	τ (μs)	FOM ($\%^2/\mu\text{s}$)
UNCL-I Passive BWR	24 ^3He tubes 4 Rectangular banks 41.4 x 16.5 x 23.4	0.59	N/A	N/A	N/A	16.3%	51	5.2
UNCL-II Passive BWR	20 ^3He tubes 4 Rectangular banks 41.3 x 16.5 x 16.5	0.49	N/A	N/A	N/A	19.1%	54	6.8
GE Reuter-Stokes ABUNCL Passive BWR	72 ^{10}B -lined tubes 4 Rectangular banks 78.1 x 16.5 x 23.4	NA	12.1% ^{##} 11.6% ^{###}	65.6 ^{##} 75.2 ^{###}	2.23 ^{##} 1.8 ^{###}	13.4% ^{##}	71.4 ^{##}	2.5 ^{##}

From [Rogers 2012b]

From [McKinny 2012]

From [Kouzes 2012b]

Additional measurements were performed of the die-away time of the passive ABUNCL configuration after the results previously reported in [Kouzes 2012b]. For these additional measurements, a Canberra JSR-14 shift register was used with the Neutron Multiplicity Counter (NMC) code from Los Alamos National Laboratory [Harker 2001]. The method was to use a fixed gate width of 16 μs , vary the pre-delay from 4 μs to 256 μs , and measure the reals-rate. The resulting die-away time from fitting this data was 76.3 μs , in reasonable agreement with the previously reported value of 75.2 μs .

Averaging the three best measurements of die-away time using the pre-delay value (76.3 μs) and the gate fit (72.8 μs) and gate ratio (78.8 μs) methods presented in the previous report gives a value of 76(3) μs for the die-away time of the passive ABUNCL.

¹ All modeling results referenced in this report were performed using the Monte Carlo N-Particle (MCNPX) [Pelowitz 2011] code.

3. ^{10}B -lined ABUNCL Active Configuration Testing

The GE Reuter-Stokes ABUNCL was shipped to PNNL in November 2012, was assembled in Building 3420, room 1304, and was tested in passive mode as previously reported [Kouzes 2012b]. One of the smallest of the four slabs of the ABUNCL was replaced with a HDPE block designed to hold an AmLi neutron source, as shown in Figure 3.1. The ^{252}Cf neutron source used for testing (56595-130E) was 1.8 μCi with an uncertainty of $\sim 5\%$ [$7.8(4)\times 10^3$ neutrons/s] on the date of use, which was adequate for this test.

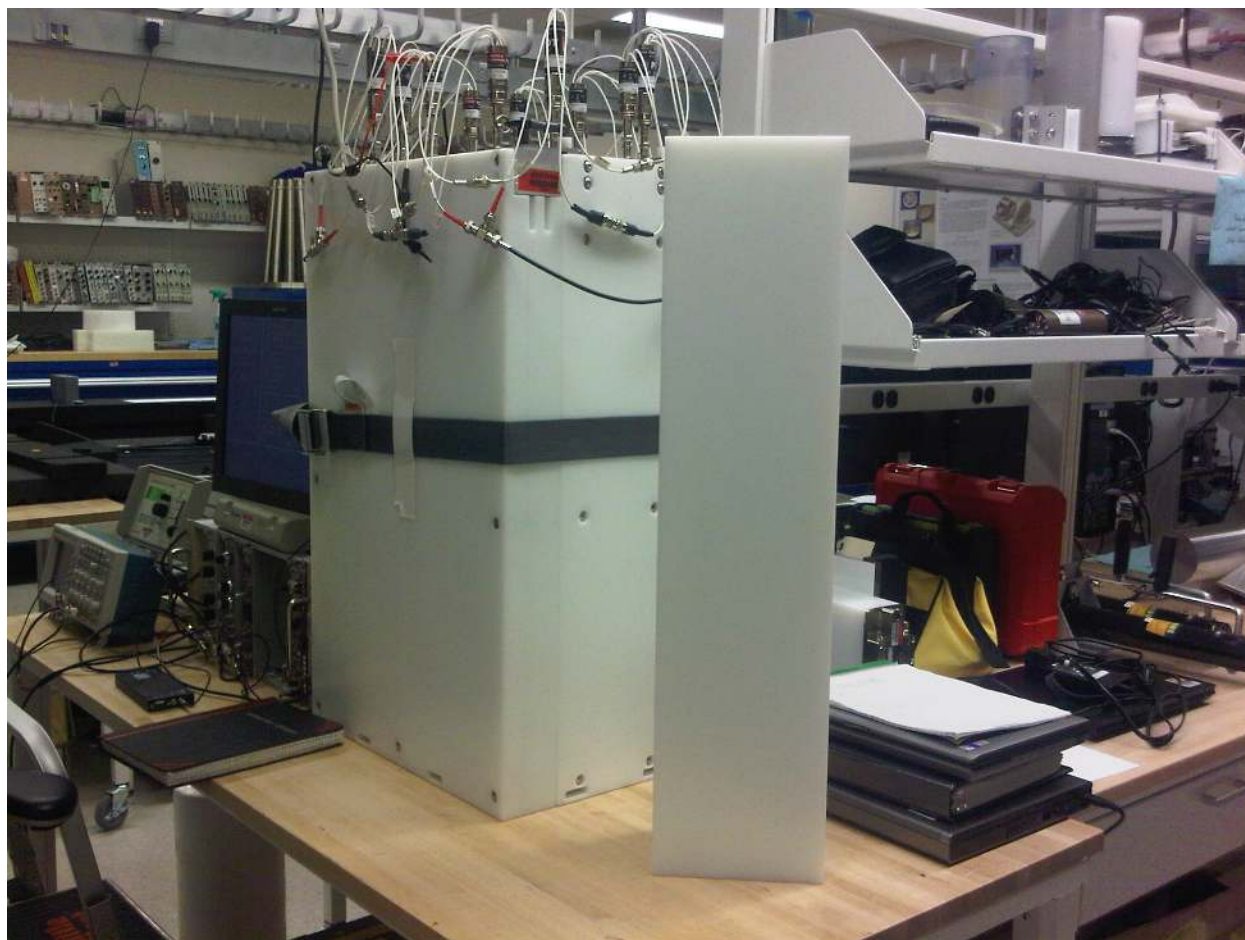


Figure 3.1. GE Reuter Stokes ABUNCL with HDPE Block to Replace Side #2.

Efficiency Measurement

The bare neutron source was positioned in the center of the ABUNCL assembly for determining the efficiency. The AMSR 150 shift register was used for the measurement. The efficiency (ϵ) of the active ABUNCL configuration was measured to be 9.4(5)%, as compared to the 11.6(3)% measured for the passive ABUNCL configuration. The uncertainty is dominated by the source strength uncertainty.

Die-Away Time Measurements

Three methods were used to determine the die-away time (τ) for the ABUNCL: the double gate ratio method, the gate variation method, and the pre-delay variation method.

Double Gate Ratio Method

The double gate ratio method and the gate variation method utilize the relationship:

$$R \sim e^{-p/\tau} (1 - e^{-G/\tau}) \quad \text{Equation 3.1}$$

where R is the real time-correlated coincident neutron detection rate, or the reals rate, p is the pre-delay length and G is the gate length. Taking the ratio of two reals rate measurements for gate lengths $G_2 = 2G_1$ and solving for τ gives:

$$\tau = -G_1 / \ln(R_2/R_1 - 1). \quad \text{Equation 3.2}$$

Table 3.1 provides the data obtained for the active ABUNCL configuration holding the pre-delay time at $4 \mu\text{s}$ and varying the gate width from 40 to $160 \mu\text{s}$. The AMSR 150 was used for these measurements. Data were collected for 100 s for each point. The pair computed die-away time is obtained using Equation 3.2, for the data in Table 3.1. The computation can only be performed for pairs, which is why the last four cells are empty. The average of all five ratios gives $78.8 \mu\text{s}$, and is $76.3 \mu\text{s}$ if the gate value for $50 \mu\text{s}$ is excluded.

Table 3.1. Gate variation data for active configuration die-away time measurement.

Gate (μs)	Total Rate	Reals Rate	Pair-Computed Die-Away Time (μs)
40	731.9	34.7	72.7 [for 40/80]
50	728.2	40.11	88.6 [for 50/100]
60	731.9	44.63	81.1 [for 60/120]
70	732.5	50.46	78.2 [for 70/140]
80	729	54.72	73.2 [for 80/160]
100	729.9	62.92	
120	731.4	65.93	
140	728.7	71.07	
160	730.2	73.06	

Gate Variation Method

The gate variation method fits the same measured reals-rate data shown in Table 3.1 to the exponential function of Equation 3.1 with the pre-delay constant at $4 \mu\text{s}$ while varying the gate width. A plot of the data is seen in Figure 3.2 with a fit giving a die-away time of $76.2 \mu\text{s}$. The uncertainty for the data points is similar to the data marker size. This is consistent with the double gate ratio method (if the gate value for $50 \mu\text{s}$ is excluded).

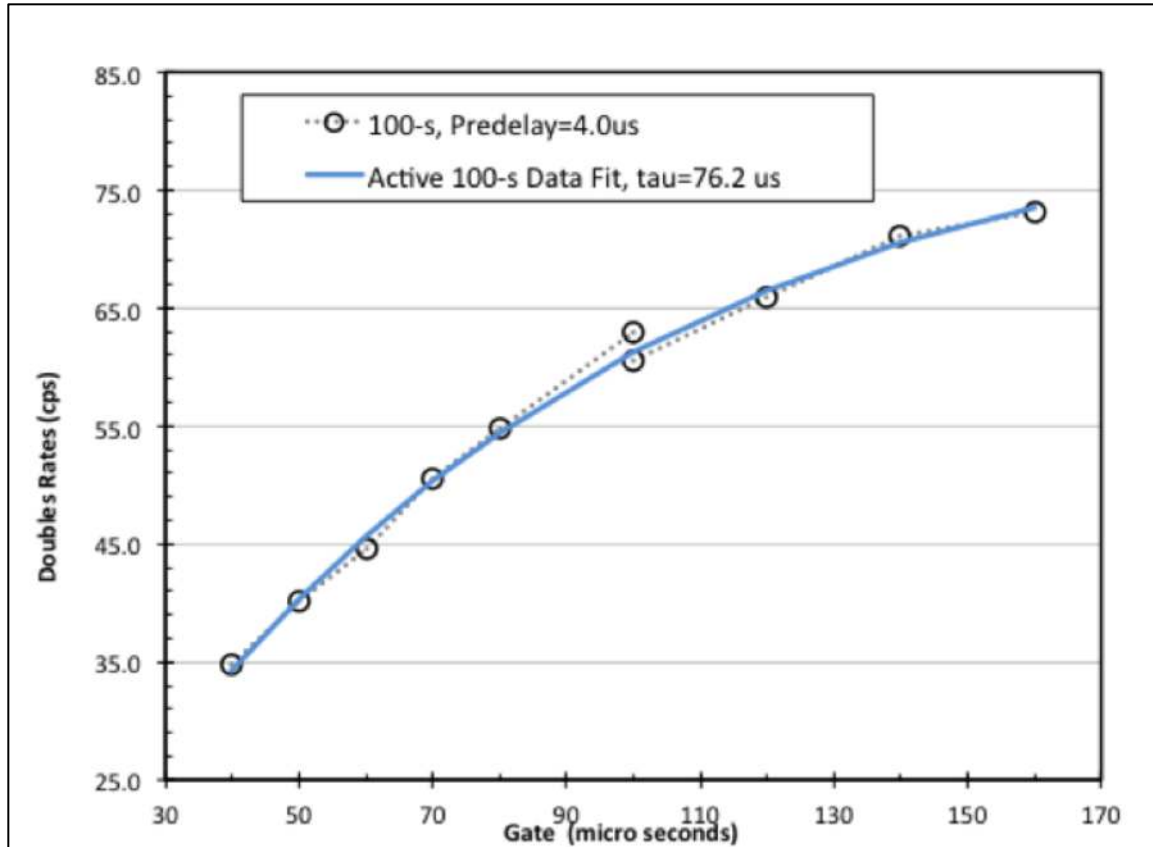


Figure 3.2. Doubles rate versus gate width fit for ABUNCL die-away-time.

Pre-delay Variation Method

The pre-delay variation method uses data taken with a constant gate width while varying the pre-delay time. The exponential in Equation 3.1 is fit to the data. Table 3.2 lists the data obtained with 100 s collection period per point and a fixed gate width of 16 μ s using the JSR-14 shift register to acquire the data. The 16 μ s gate was chosen to be short compared to the die-away time.

Table 3.2. Pre-delay data for active configuration die-away time measurement.

Pre-delay (μ s)	Total Rate	Reals Rate
4	725.6	15.04
8	731.7	14.09
16	729.6	12.949
32	732.2	11.308
40	724.8	10.638
48	724.9	9.657
56	722.2	7.055
64	728.6	7.586
128	722.2	3.382
256	723.3	0.881

Figure 3.3 shows a fit to the doubles rate versus pre-delay data, with a resulting die-away time of 87.9 μs . The graph also shows the curve for a 76.2 μs die-away time that was found in the gate width method. It is not clear why there is such a different result for the die-away time from the gate width method (76.2 μs), gate ratio method (78.8 μs), and the pre-delay method (87.9 μs), but one of the potential contributions to the discrepancy is addressed below.

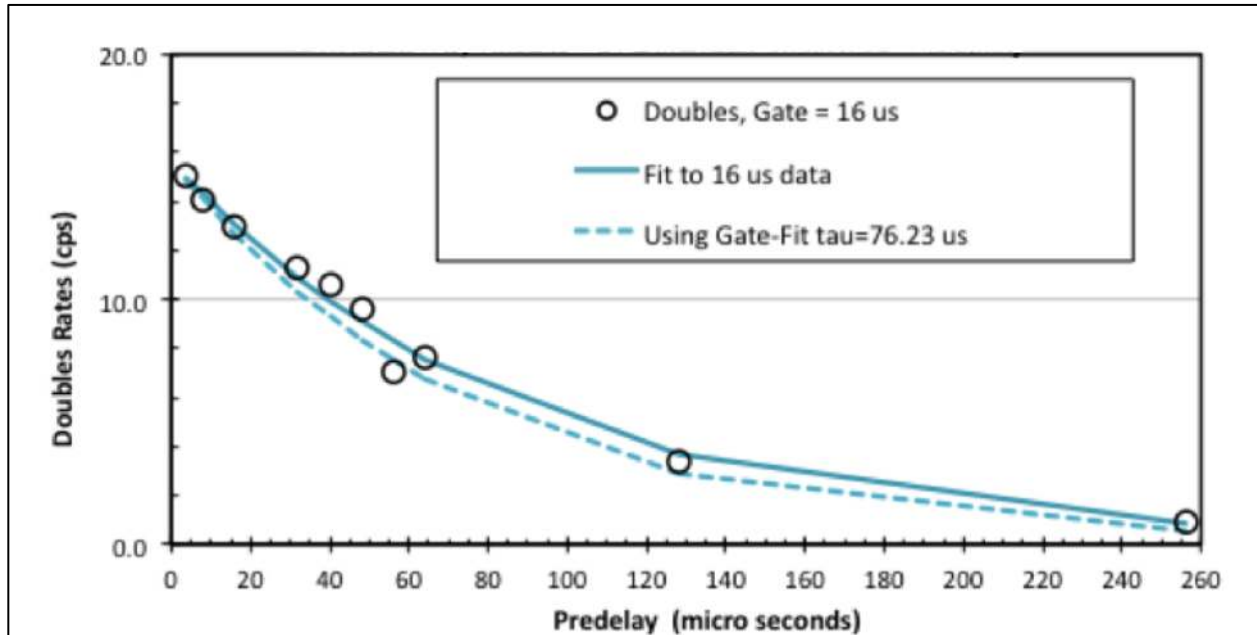


Figure 3.3. Doubles rate versus pre-delay fit for die-away-time.

Repeat of Die-Away Time Measurements

One of the sources of error in the results given above was that two different instruments were used to acquire the data (AMSR 150 for the gate methods and JSR-14 for the pre-delay method). Another data set was accumulated using the JSR-14 for all data collection.

Table 3.3 provides the data obtained using the JSR-14, where the gate width was varied from 16 to 128 μs and the pre-delay was varied from 4 to 128 μs .

These data were analyzed using both the gate variation and pre-delay variation methods. Figure 3.4 shows the fits to the data for the gate variation method for various values of the pre-delay, while Figure 3.5 shows the fits to the data for the pre-delay variation method for various values of the gate width.

The average of the gate width variation method for all the pre-delay values gives a die-away time of 86(8) μs . Excluding the two longest pre-delay values (64 and 128 μs), which are long compared to the die-away time and are trending to larger values, gives a value of 82(3) μs .

The average of the pre-delay method fits to the die-away time is 84(4) μs .

Averaging these consistent values from the two methods gives a die-away time of 83(3) μs . This value falls in the middle of the values obtained from the previous measurements, and will be taken as the die-away time for this active ABUNCL configuration.

Table 3.3. Data for active configuration die-away time measurement.

Pre-delay (μs)	Gate (μs)	Total Rate	Doubles Rate
4	16	727.3	14.93
8	16	722.8	14.7
16	16	725.8	13.55
32	16	723.9	11.3
48	16	723.5	8.73
64	16	726.8	7.34
128	16	723.5	3.38
4	32	724.8	27
8	32	726.5	27.4
16	32	720.9	23.8
32	32	721.7	19.9
48	32	724.6	15.4
64	32	724.7	12.7
128	32	724.1	5.83
4	64	723.9	46.3
8	64	723	45.69
16	64	729.2	41.3
32	64	723	34.2
48	64	725.5	28.1
64	64	726.2	22.6
128	64	718.6	11.1
4	128	717	67.79
8	128	723.7	64.55
16	128	720.3	60.62
32	128	719.6	49.53
48	128	721.8	38.26
64	128	722.4	33.49
128	128	727.8	16.05

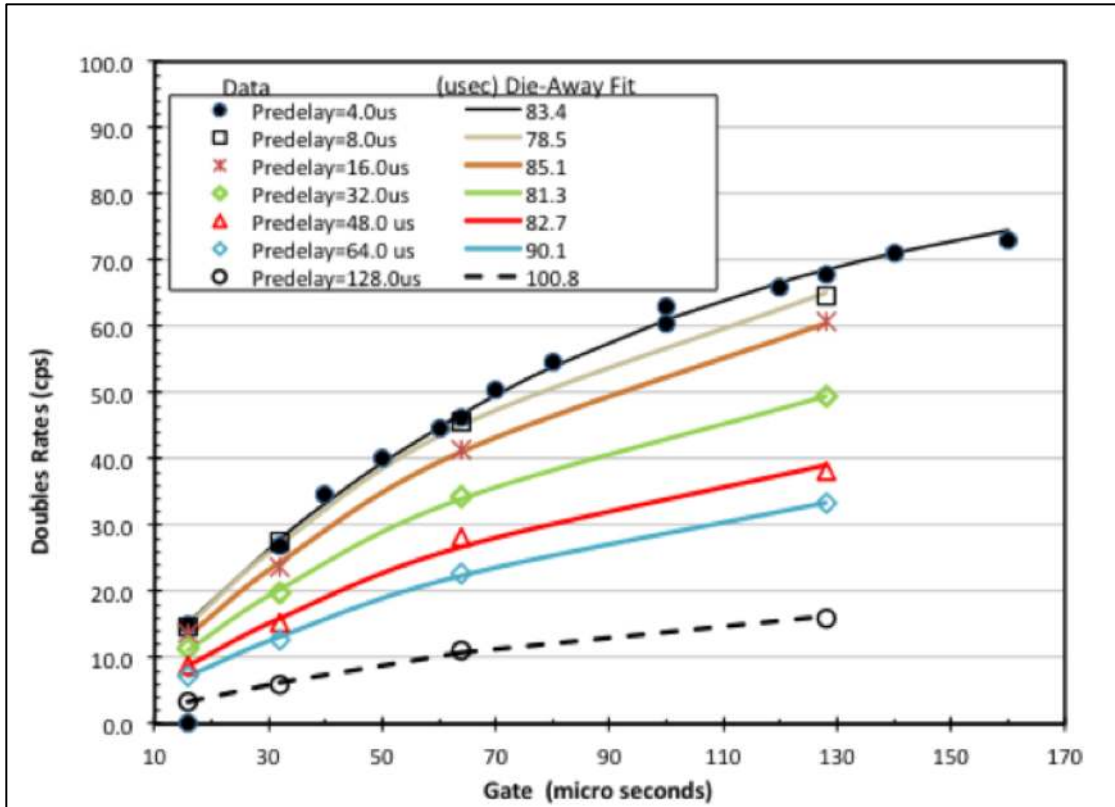


Figure 3.4. Doubles rate versus gate width fit for die-away-time.

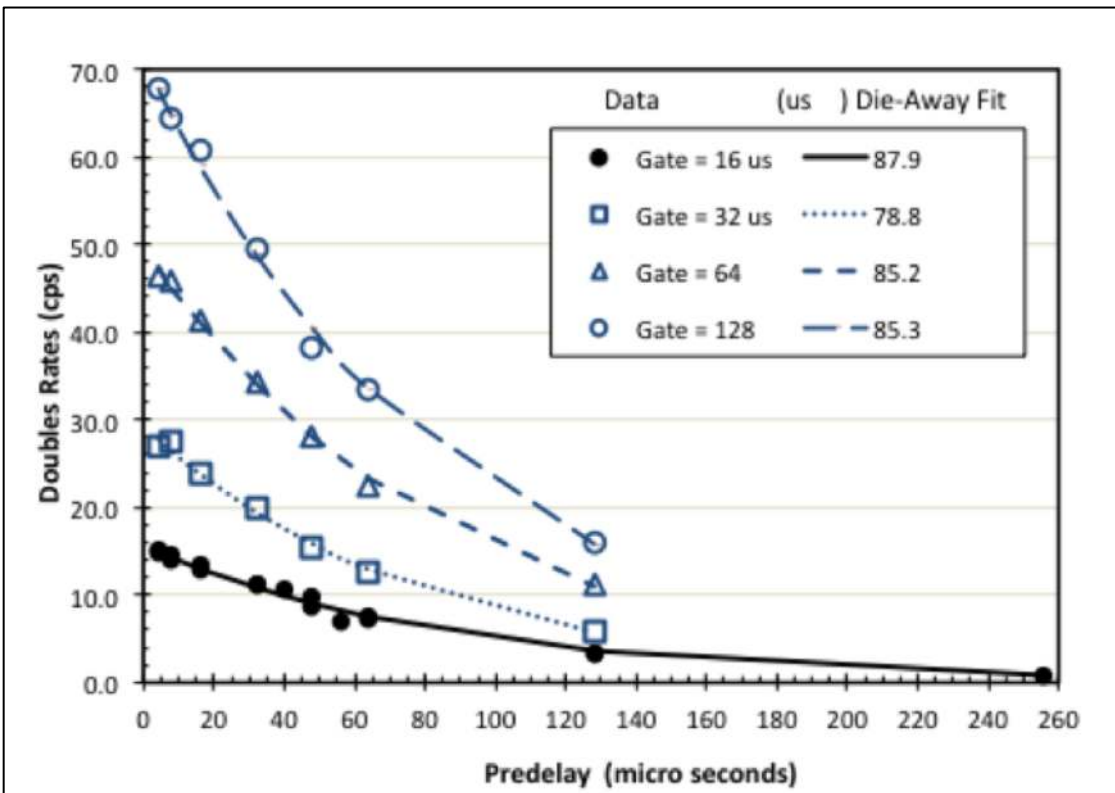


Figure 3.5. Doubles rate versus pre-delay fit for die-away-time.

AmLi Measurements

Measurements were made with an AmLi source (#9975), which emits $2.5(3) \times 10^4$ neutrons per second. The source was placed in the center of the passive ABUNCL and the efficiency was measured to be 12(1)%. This efficiency may be higher than that obtained with the ^{252}Cf source due to the lower energy spectrum from AmLi. The uniformity of efficiency with energy should be a design consideration for future configurations.

The AmLi source was also placed in the side moderator source holder location, which is vertically and horizontally centered, and about 1.3 cm into the polyethylene block. The efficiency for detection for the source in this location was found to be 7.6%.

4. ^{10}B -lined ABUNCL Modeling Results

Previous work at PNNL modeled the eight configurations of the ^3He -based UNCL coincidence counter [Siciliano 2012b]. Various designs of an ABUNCL using boron-lined tubes were also modeled [Rogers 2012b].

As part of the current project effort for testing of the GE Reuter Stokes (GERS) ABUNCL design, PNNL needed to model that specific design to 1) show agreement with the modeling results previously performed by GERS (McKinney 2012), 2) compare to the PNNL testing results of that design, and 3) modify the model to evaluate the active ABUNCL configuration. For these tasks, three MCPNX models were used. The first model (named B10PNCC) was developed by GERS and provided to PNNL under a non-disclosure agreement. The second passive model (named GEUNCL-P) was a revised version of the GERS model used for most of the results listed below. The third model (named GEUNCL-A) was the active version of the GEUNCL-P model. Because the B10PNCC model provided by GERS had the information about their boron lining composition removed, the modeling tasks at PNNL were performed with various lining compositions to compare to those in the GERS reference (McKinney, 2012). A more detailed discussion of these three models and their results is discussed below.

To coordinate the modeling efforts at PNNL with that already performed by GERS, an input file named "B10PNCC.i.i" was received by PNNL on 10 December 2012 from Nathan Johnson of GERS. Per the non-disclosure agreement between PNNL and GERS concerning this coordination, this file was described by Johnson to be a "simplified" version, presumably removing all proprietary details not covered under that non-disclosure agreement. From previous discussions with, and materials received from GERS, this simplification was expected to affect certain details of the model for the boron lining. Indeed, the only component listed in the B10PNCC.i.i file that was commented explicitly as having been "simplified" was the material used for the boron lining composition. It was specified to be 100% ^{10}B and used at the elemental density of 2.34 g/cc. The other important modeling detail of the boron lining, i.e., the thickness, was not indicated as simplified, and was assumed by PNNL to be the same as in the original GERS version of the B10PNCC model. Those values were given as 2.65 μm for the 32 outer tubes and 1.65 μm for the remaining 38 inner tubes.

Examination of other geometries (particularly the amounts of HDPE) and fill gas details in the B10PNCC.i.i file were observed to be inconsistent with information previously provided by GERS about their ABUNCL counter and their boron-lined tubes. References to those details include the engineer drawing labeled "SK-3141-82 Rev 01.pdf," received 18 October 2012, the GERS brochure for the 1"x24" boron-lined tube model RS-B1-0824-101 (assumed used in the test counter), private communications with GERS about their (1"-diameter) boron-lined tubes, and details shown in GERS 2012 IEEE paper [McKinney 2012]. These discrepancies included: omissions of air-gaps outside of the tube walls; omission of the dead-zone volumes at the ends of the tubes; use of 100% Ar at 1 atm. pressure instead of the 90%-10% Ar-CO₂ blend at a lower pressures (as stated by GERS in their advertisement brochures and private communications); and excess volumes of HDPE at the bottom and top of the counter.

The effect of correcting the discrepancies mentioned above were evaluated by revising and recoding the B10PNCC model into a PNNL version called the GEUNCL-P model, for the GE

UNCL Passive model. By evaluating individually the effect of each change, it was found that the only significant effect was a reduction in count efficiency and die-away time from correcting the amounts of HDPE at the top and bottom of the model. The size of that reduction effect can be seen in the side-by-side list of performance parameters given in Table 4.1 for the B10PNCC and GEUNCL-P “BL & Pig” results. The “Pig” refers to Pb and steel shield around the source that was part of the as-delivered B10PNCC model and it was used only for that column of GEUNCL results. Here, as with all following results, the model performance parameters are listed with various low-energy cutoff (LEC) values for the boron-metal lined (BL), boron-carbide lined (B₄C), and boron nitride (BN) lined tubes. The total capture efficiency is the probability of a neutron being captured in the detector lining, while the efficiencies as a function of thresholds are those for observing a signal. Most of the modeled efficiencies are larger than the measured value of 11.6% (100 keV cutoff). Details of the B10PNCC model (from which the GEUNCL was built) are shown pictorially in Figure 4.1.

Table 4.1. Results for simplified B10PNCC model compared to PNNL revised version GEUNCL-P.

Model ==>	B10PNCC	GEUNCL-P	GEUNCL-P	GEUNCL-P	GEUNCL-P
	BL & Pig	BL & Pig	BL	B₄C	BN
	ε (%)	ε (%)	ε (%)	ε (%)	ε (%)
Total Capture Efficiency	33.9	30.2	29.5	34.7	49.8
LEC (keV)					
0	20.0	16.9	16.4	14.9	11.4
50	18.7	15.8	15.3	13.9	10.6
100	17.7	15.0	14.5	13.2	10.0
150	17.0	14.3	13.9	12.6	9.5
	τ (μs)	τ (μs)	τ (μs)	τ (μs)	τ (μs)
Die-Away Time	76.5	76.1	75.9	83.9	100.7

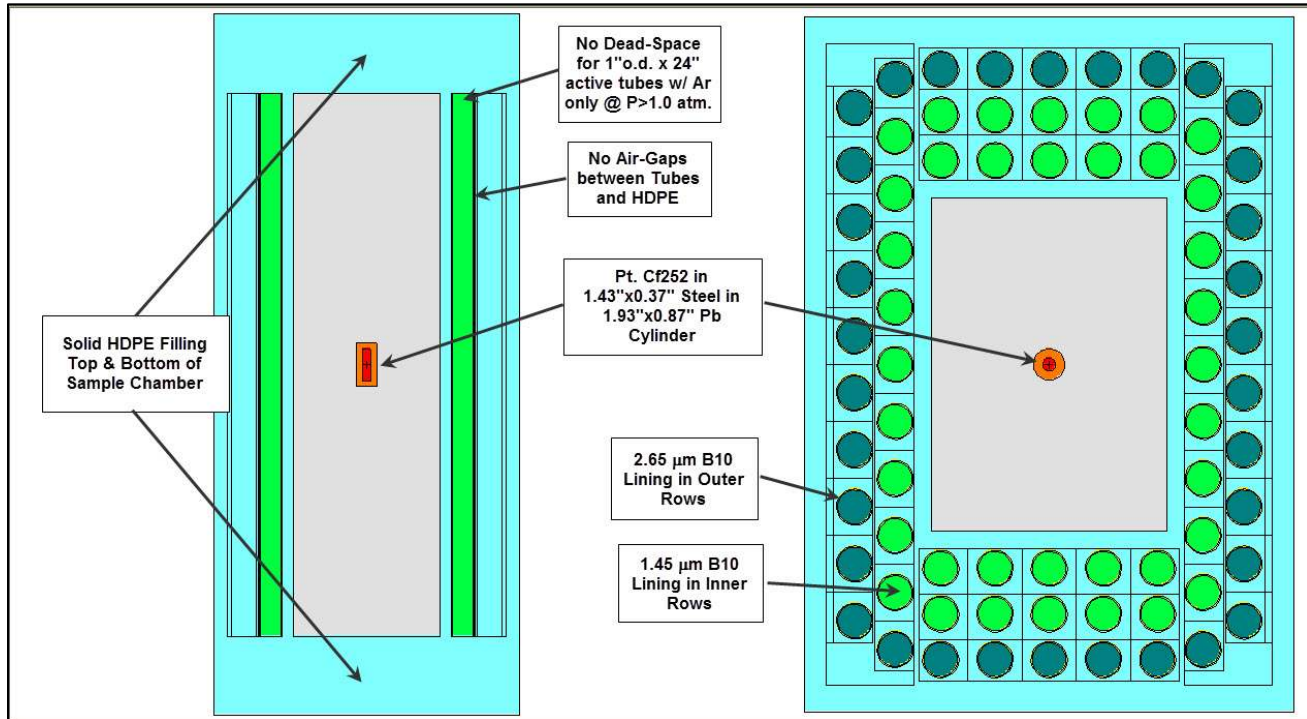


Figure 4.1. Side (left) and top (right) cross-sectional views of the B10PNCC model from GERS.

The cross-sectional views in Figure 4.1 were taken through the center of the counter, and although each view shows correct relative geometries of the components, the top (right side) view was enlarged by about 60% with respect to the side (left) view. In these screen captures, the light blue areas are filled with HDPE and the light gray area is air-filled. The outer (dark green) and inner (light green) rows of tubes have different lining thicknesses. Note that the top view screen capture in this figure is, except for annotations and coloring, identical with one in the GERS 2012 IEEE paper [McKinny 2012].

The results for the B10PNCC model were computed “as delivered,” with the source particles emitted from the center of the afore-mentioned “Pig,” i.e., the Pb-wrapped steel cylinder shown in Figure 4.1. That model also used a one-parameter Maxwell distribution for the spontaneous fission neutrons from a ^{252}Cf point source (versus the more recent two-parameter Watts form, MCNPX manual, Appendix H). Because no corresponding output or analysis files were sent by GERS, it was concluded that the only unambiguous tallies from that output file were the tally types F8 for the pulse heights of the alpha and lithium reaction products in the fill gas volumes of the tubes. The sums of those resulting values from the B10PNCC output were given in two energy bins, from zero to 145 keV and from 145 keV to 3 MeV. In terms of percentage counting efficiencies, they were found to be 3.0% and 17.0%, respectively, giving the total for the full-energy range (i.e., no LEC) to be 20%.

For a more complete set of results from the B10PNCC model, the tally options were changed to conform to those used in previous studies for modeling of boron-lined alternative detector configurations [Kouzes 2012b]. Those changes of tally options allowed for the same set of customized analysis workbooks to be used to obtain a consistent and complete set of analyses of the B10PNCC results. They included the efficiency rates for neutron capture in the linings using

tally type F4 with a FM4 option for capture cross-sections; and correlated energy depositions of the reaction products in the gas using tally type F8 PHL with type F6 tracking of the products. Both of those calculations were obtained as a function of time and to find the corresponding die-away times by fitting to a single exponential shape. Figure 4.2 shows the die-away time analyses for the B10PNCC model showing different fits to neutron capture counts in the lining to the correlated energy deposition of reaction products in the proportional gas. Figure 4.3 shows the pulse-height spectra for individual reaction products and the total in 1-atm. Ar tube fill gas.

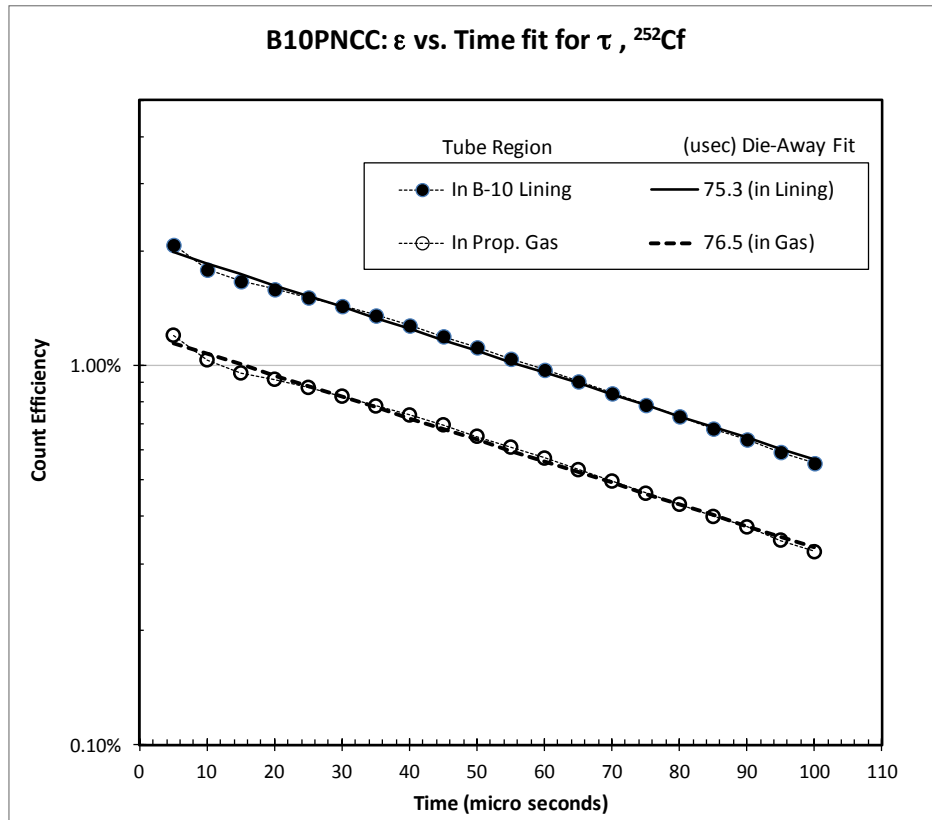


Figure 4.2. Die-away time analyses for the B10PNCC model.

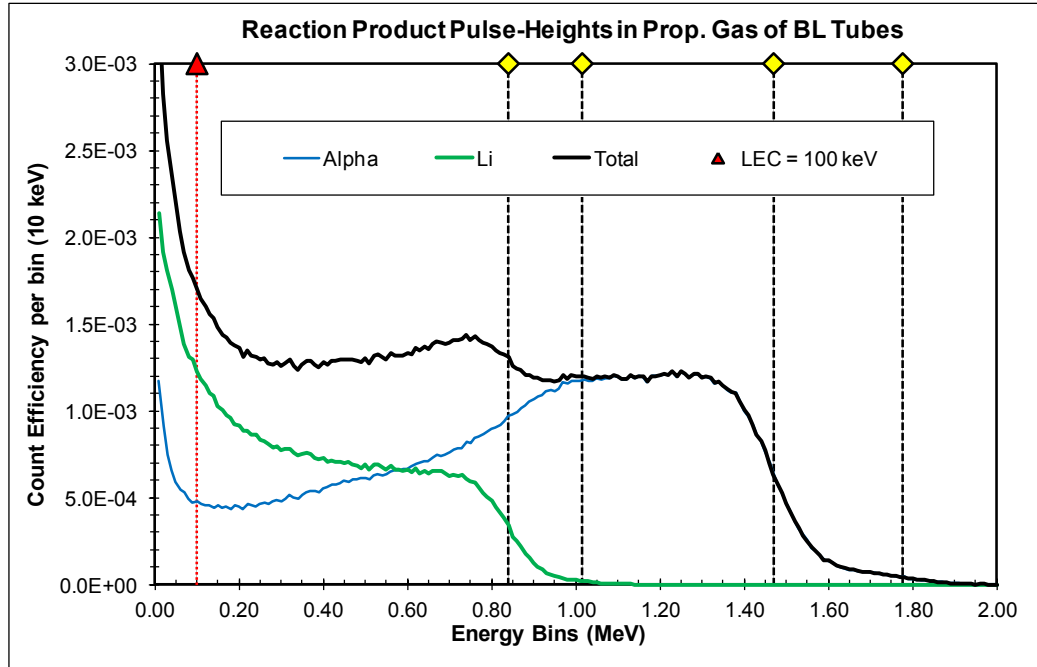


Figure 4.3. Pulse-height spectra for individual reaction products and total.

As seen in Figure 4.2, the magnitude of the total capture efficiency of neutrons in the lining is larger (as it should be) than that of the energy deposition in the proportional gas, which is the model result for the modeled total counting efficiency (ϵ). The time dependence of those two related processes are approximately equal. The PNNL analysis workbooks also provide numerical values of ϵ for user-selected values of the LEC threshold. Values for ϵ are distinguished from the values for total capture efficiency, for which there is no threshold. For LEC values of 0, 50, 100, and 150 keV, the numerical values of ϵ for the pulse-height spectrum shown in Figure 4.3 were evaluated to be 20.0%, 18.7%, 17.7% and 17.0%, respectively. As expected, the LEC 0 and 150 keV values are the same as found using the “as delivered” total and 145 keV LEC results mentioned above. The value for the total capture efficiency was 33.9%, which in ratio to the 20% ϵ value is the scaling between the two time-dependent results shown in Figure 4.2.

As stated above, it is assumed that the lining material composition was the only significant difference between the B10PNCC model delivered to PNNL and that used by GERS to model their as-built test counter. Although there were no other files delivered along with the simplified B10PNCC model, it is possible to use GERS modeling results presented in their 2012 IEEE reference [McKinny 2012]. In that reference, two sets of modeling results for efficiencies and die-away times were listed. The first set, labeled as “optimized” were 14.3% and 81 μ s, respectively, obtained using a ^{10}B loading of 0.48 mg/cm^2 for the thicker linings and 0.28 mg/cm^2 for thinner linings. The second set of model results were labeled as “as built,” and were given as 13.4% and 71.4 μ s, respectively, for a “built-up” ^{10}B loading of 0.62 mg/cm^2 for the thicker linings and 0.34 mg/cm^2 for the thinner linings. The second set of results was compared to reported measured values of 12.1% and 65.6 μ s. All of these were for a National Institute of

Science and Technology (NIST) calibrated ^{252}Cf source, embedded in the Pb-wrapped steel cylinder shown in Figure 4.1. From these modeling results, the values of the lining thickness (1.45 μm and 2.65 μm) in the as-delivered 10BPNCC model can be verified, supporting the assumption that the only difference is in the lining material composition. Note that the model results overestimate the measured efficiency and die-away time, which is a typical behavior for too much moderation. The size of the change for correcting this discrepancy between the B10PNCC model and the as-built counter is given below in the results for the GEUNCL-P model.

It is a simple exercise to evaluate the lining thickness values corresponding to 100% ^{10}B material at the above stated values of ^{10}B loadings. Using the symbol sigma (σ) for areal density in mg/cm^2 and T for thickness, the values for T in units of microns are then: $T = \sigma/0.234 \text{ mg}/\text{cm}^3$. This gives T values of 2.05 and 1.20 microns for the “optimized” loading values; and 2.65 and 1.45 microns for the “built-up” loading values. Note that the latter set of values are the same as those used in the simplified B10PNCC model, and thus the proper values of efficiency and die-away time to compare to in estimating the effect of the simplified lining composition are the 13.4% and 71.4 μs results given in the 2012 IEEE reference [McKinny 2012].

A screen capture of the side view through the center of the GEUNCL model is shown in Figure 4.4, juxtaposed, but not exactly to the same scale, to the referenced GERS engineer drawing of the test counter. Besides recoding the MCPNX input to comply with evaluation methods for consistency with previous studies at PNNL, the GEUNC model includes small air gaps outside of the tube side walls (not visible), gas-filled dead zones at the end of the tubes, and, reduction in the HDPE (light blue) volumes at the top and bottom of the counter. In this, and additional screen captures of the GEUNCL model, the color of the gas-filled volumes are linked to the gas material, and will be shown in red for all the tubes. Recall for descriptive purposes, the colors used in Figure 4.1 were linked to the lining thickness values. Also note that the engineering drawing shown in the figure appeared in the referenced GERS 2012 IEEE paper [McKinny 2012].

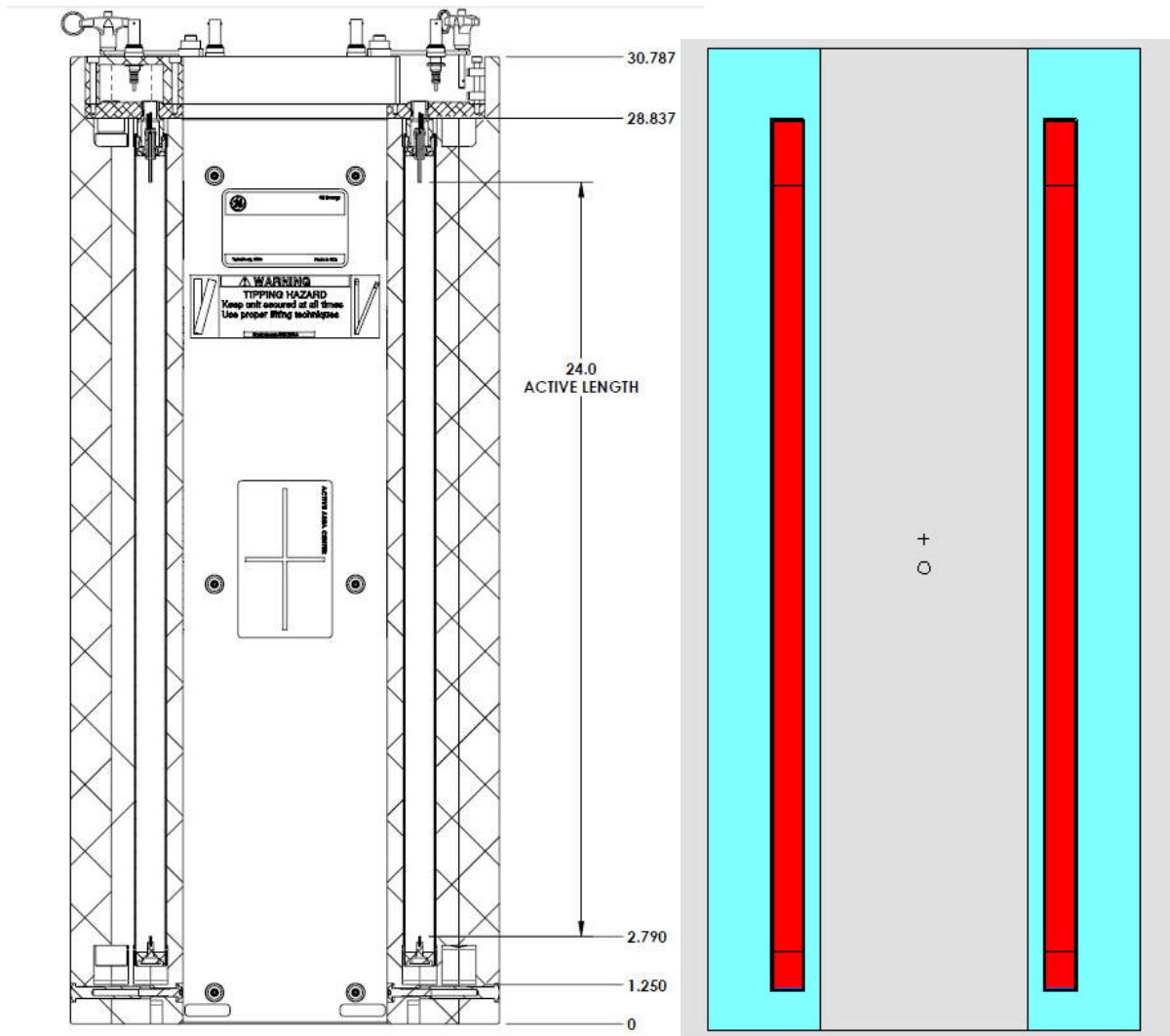


Figure 4.4. Comparison of GERS Drawing and GEUNCL upgrade to B10PNCC configuration.

Additional screen captures showing side and top views through the centers of the passive GEUNCL-P, and the active version, GEUNCL-A, are given in Figures 4.5 and 4.6. As with the screen captures of the B10PNCC model shown in Figure 4.1, each view shows the correct relative geometries of the components, but the top (right side) view was enlarged by about 60% with respect to the side (left) view.

In Figure 4.5, the side cross-sectional view is the same as shown in Figure 4.2, but now also includes the 10 source positions used for the vertical source position profile calculations for both the passive and active GEUNCL models (results shown in Figures 4.7 and 4.8 at the end of this section). The top cross-sectional view in Figure 4.5 is for the active version of the GEUNCL model, where the 15 tubes in the front polyethylene block have been replaced by a solid block, flush with the outer dimensions of the counter, but with a 3.50-cm diameter 43.18-cm deep active source placement hole. The depth of that hole is shown in the left side of Figure 4.6, where that side view cross section was taken through the center of the access hole. The top view

in that figure is the same as the one in Figure 4.5, but now shows the first 1000 collision sites occurring throughout the total height of the counter for the AmLi source in the hole.

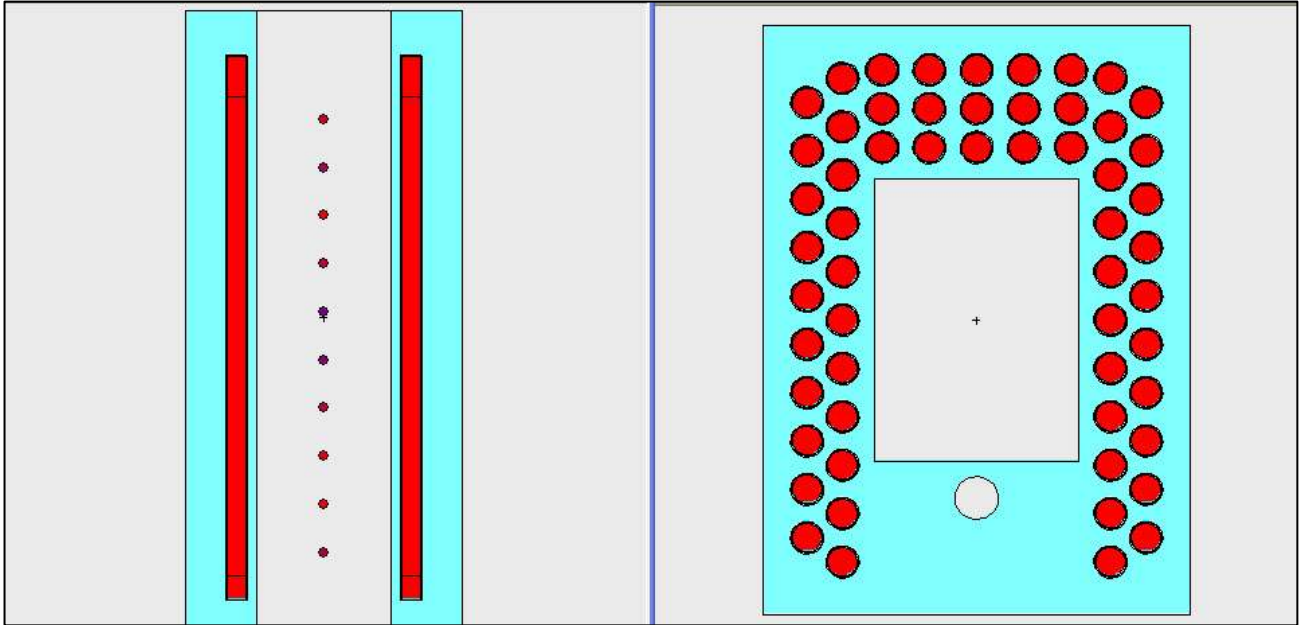


Figure 4.5. Left side is side cross-sectional view showing positions for the vertical source profile calculations. Right side is top cross-sectional view through center of active GEUNCL model.

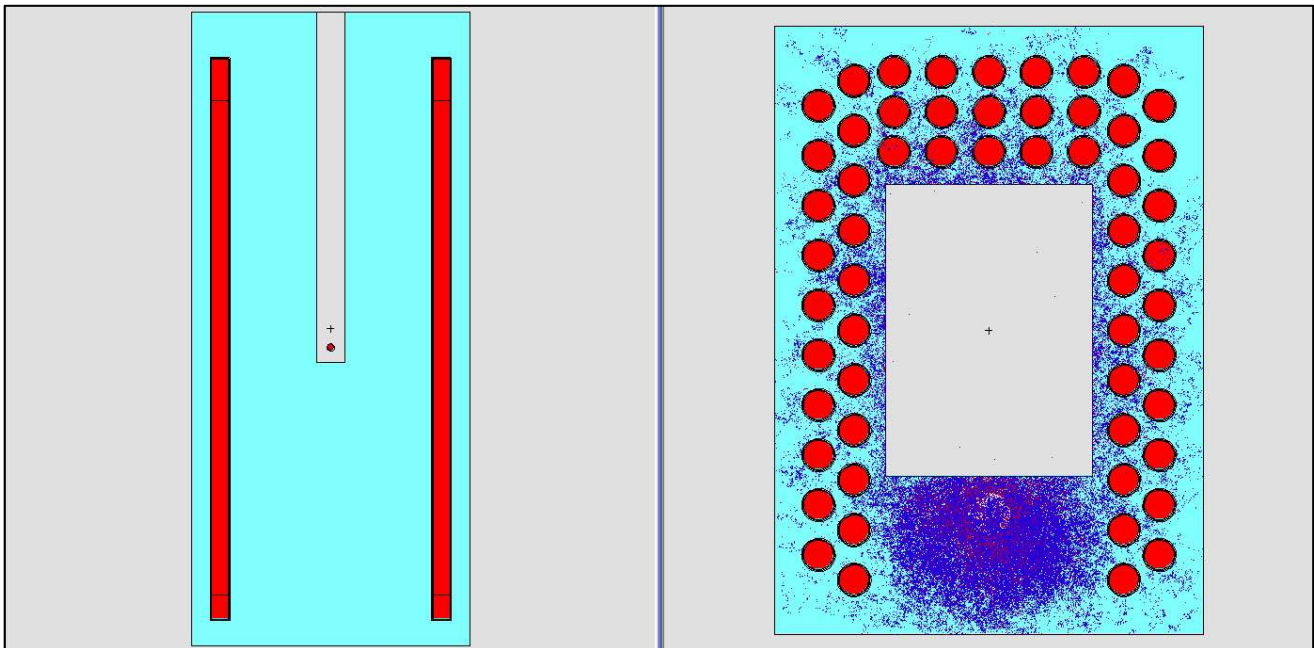


Figure 4.6. Side (left) and top (right) cross sectional views of active GEUNCL model.

Results for the count efficiencies and die-away times for the three different model configurations evaluated in this study, i.e., B10PNCC, GEUNCL-P, and GEUNCL-A, are listed in the following tables using the same methods of analyses described for Figure 4.2. The results from all three models were obtained using a fill-gas of 100% Ar at 1-atm. and 20°C. The effect of changing the fill gas to a 90%-10% blend of Ar-CO₂ at 0.33 atm. was evaluated and found to give a very small reduction in the efficiency and die-away times, which resulted from a correspondingly small wall effect on the alpha pulse height in 2.54 cm diameter tubes. Unless otherwise stated (e.g., in the third column of Table 4.1), all the GEUNCL models used the two-parameter Watts distribution for the ²⁵²Cf source without the Pb-Steel “Pig.” Table 4.2 shows effects of changes in boron lining materials and thickness in GEUNCL-P model.

Table 4.3 shows results for the PNNL active model version, GEUNCL-A. Table 4.4 shows effects of changes in boron lining materials and thickness in the GEUNCL-A model.

Table 4.2. Effects of changes in boron lining materials and thickness in GEUNCL-P model

Model ==>	GEUNCL-P	GEUNCL-P	GEUNCL-P	GEUNCL-P	GEUNCL-P	GEUNCL-P
	1.45 μm BL	1.45 μm B ₄ C	1.45 μm BN	2.65 μm BL	2.65 μm B ₄ C	2.65 μm BN
	ε (%)	ε (%)	ε (%)	ε (%)	ε (%)	ε (%)
Total Capture Efficiency	27.1	31.5	44.5	32.4	38.5	56.2
LEC (keV)						
0	17.5	15.8	12.2	14.7	13.5	10.2
50	16.3	14.8	11.4	13.6	12.5	9.4
100	15.5	14.1	10.8	12.9	11.8	8.7
150	14.9	13.5	10.4	12.3	11.3	8.2
	τ (μs)	τ (μs)	τ (μs)	τ (μs)	τ (μs)	τ (μs)
Die-away Time	89.5	98.9	119.4	60.3	67.5	80.7

Table 4.3. Results for PNNL Active version, GEUNCL-A

Model ==>	GEUNCL-A	GEUNCL-A	GEUNCL-A	GEUNCL-A	GEUNCL-A
	BL	B ₄ C	BN	BL	BL
				AmLi Centered	AmLi Side
	ε (%)	ε (%)	ε (%)	ε (%)	ε (%)
Total Capture Efficiency	24.7	29.0	41.4	33.5	20.5
LEC (keV)					
0	13.6	12.3	9.4	18.8	11.8
50	12.7	11.5	8.7	17.5	11
100	12	10.9	8.2	16.6	10.5
150	11.5	10.4	7.8	15.9	10
	τ (μs)	τ (μs)	τ (μs)	τ (μs)	τ (μs)
Die-away Time	76.9	85.1	101.6	77.6	113.9

Table 4.4. Effects of changes in Boron Lining Materials & Thickness in GEUNCL-A model.

Model ==>	GEUNCL-A	GEUNCL-A	GEUNCL-A	GEUNCL-A	GEUNCL-A	GEUNCL-A
	1.45 μm BL	1.45 μm B ₄ C	1.45 μm BN	2.65 μm BL	2.65 μm B ₄ C	2.65 μm BN
	ϵ (%)	ϵ (%)	ϵ (%)	ϵ (%)	ϵ (%)	ϵ (%)
Total Capture Efficiency	22.4	26.0	36.6	27.1	32.2	46.7
LEC (keV)						
0	14.5	13.1	10.0	12.3	11.3	8.5
50	13.6	12.2	9.4	11.5	10.5	7.8
100	12.9	11.6	8.9	10.9	9.9	7.3
150	12.3	11.1	8.5	10.4	9.5	6.8
	τ (μs)	τ (μs)	τ (μs)	τ (μs)	τ (μs)	τ (μs)
Die-away Time	91.8	101.8	120.4	61.6	69.4	82.9

As mentioned above, the model used for the GEUNCL results for a ^{252}Cf source was a two-parameter Watts distribution. For the AmLi point source results listed in Table 4.3, a measured set of data was inserted as a histogram model for its emission spectrum. A comparison of the AmLi neutron emission spectrum to a comparably measured spectrum from ^{252}Cf is shown in Figure 4.7. Efficiency versus energy and versus vertical position was also evaluated and the results are shown in Figures 4.8 and 4.9. For these results, the source was modeled as a series of mono-energetic neutron point sources. It is seen from the measured spectra that the two different sources have very similar shapes, and differ mainly in energy. The efficiency is fairly flat from thermal energies to almost 1 MeV.

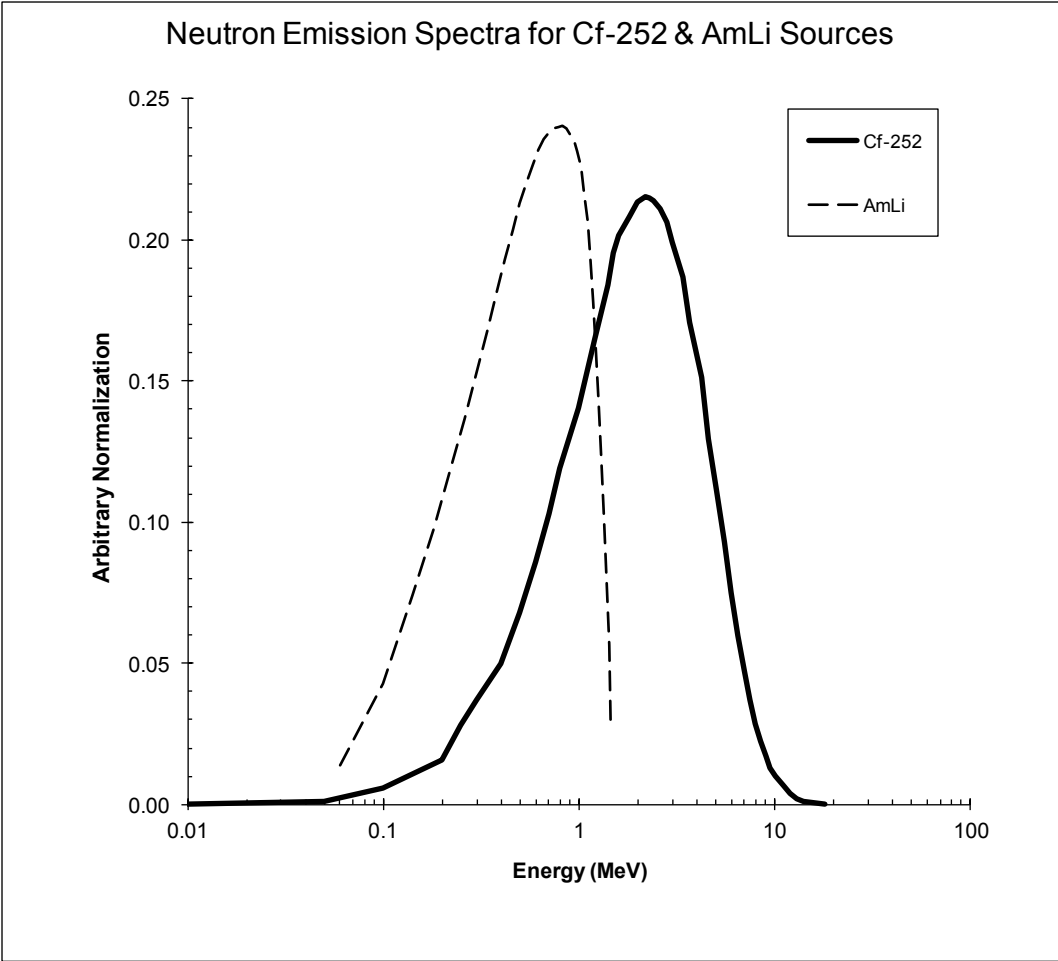


Figure 4.7. Lethargy plots of energy spectra of several neutron sources. AmLi data are from [Geiger 1971] and ²⁵²Cf data are from [ISO 1989].

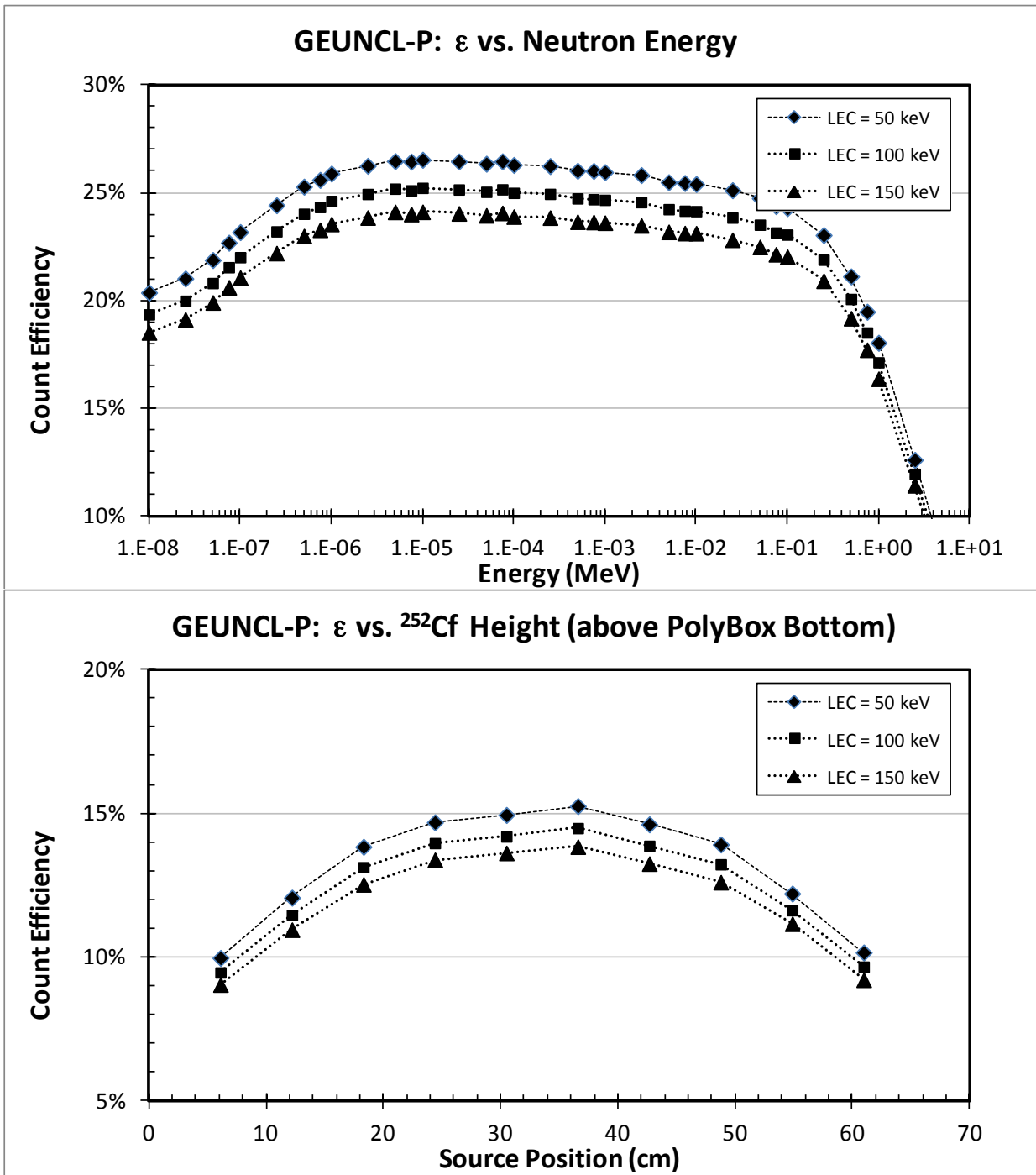


Figure 4.8. Energy (top) and source position (bottom) profiles for the passive GEUNCL-P model.

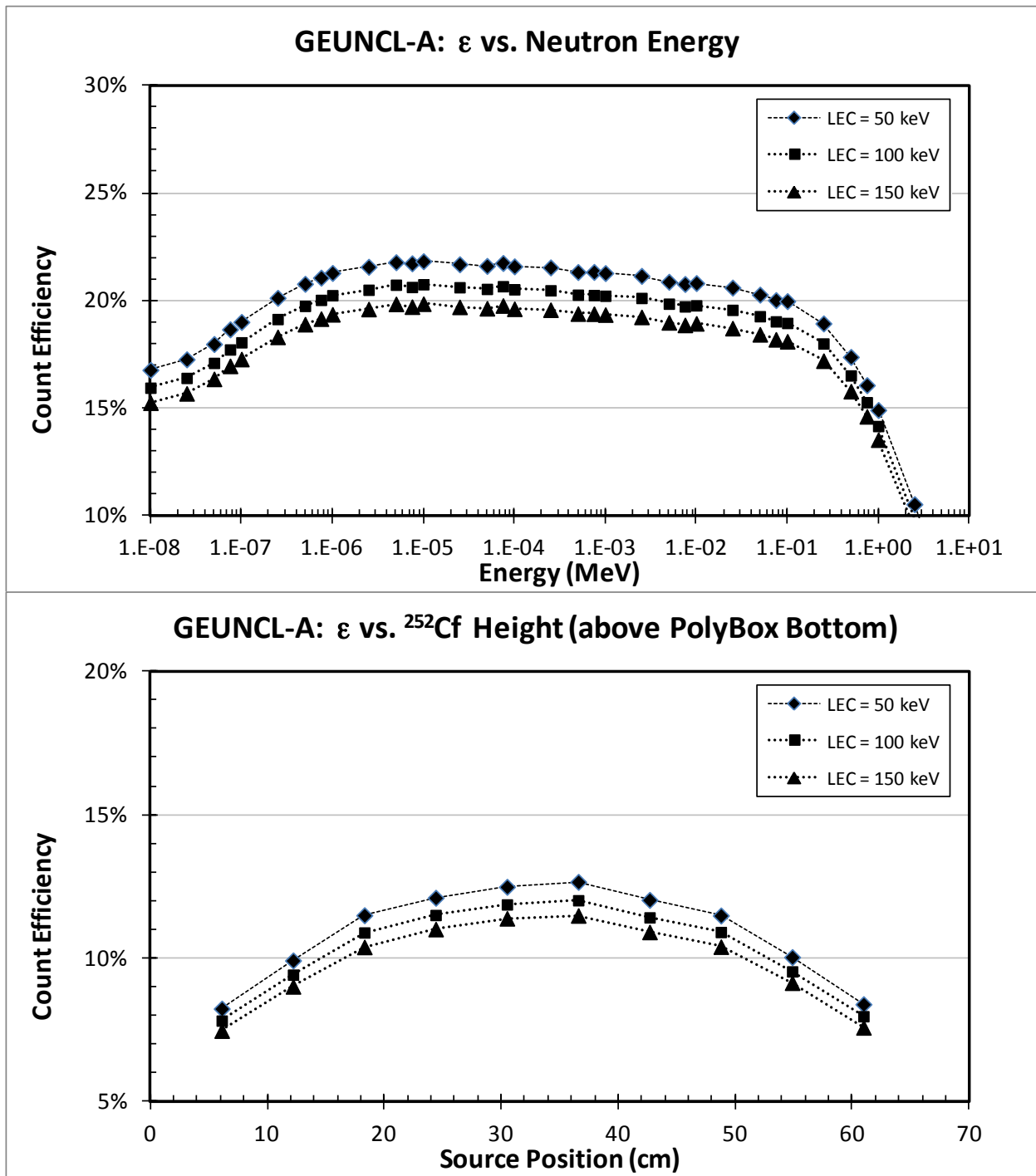


Figure 4.9. Energy (top) and source position profiles for the active GEUNCL-A model.

5. Conclusions

This report discussed the characterization of a full-scale boron-based ABUNCL coincidence counter developed by GE Reuter-Stokes for applications in safeguards for Task 2 of the project *Coincidence Counting With Boron-Based Alternative Neutron Detection Technology*.

This report provides results from MCNPX model simulations and initial testing of the active mode variation of the ABUNCL design built by General Electric Reuter-Stokes. Initial experimental testing of the as-delivered passive ABUNCL was previously reported.

The efficiency of the reconfigured *active* ABUNCL determined from measurement of a centered ^{252}Cf source was found to be 9.4(5)%, with a die-away time of 83(3) μs . This is compared to the value measured for the *passive* ABUNCL of 11.6(3)%, with a die-away time of 75.2 μs . Combining the efficiency and die-away time gives a FOM (ϵ^2/τ) of 1.1 for the active ABUNCL, compared to a FOM for the passive ABUNCL of 1.8.

The MCNPX model results of the passive configuration provided by GE Reuter-Stokes were reasonably consistent with the results reported [McKinny 2012].

6. Acknowledgements

The United States Department of Energy Office of Nuclear Safeguards and Security (NA-241) supported this work. Pacific Northwest National Laboratory is operated for the United States Department of Energy under contract DE-AC05-76RLO 1830. Azaree Lintereur is a post Masters Research Assistant supported at Pacific Northwest National Laboratory by the Next Generation Safeguards Initiative, Office of Nuclear Safeguards and Security, National Nuclear Security Administration.

7. References

- Croft S, A Favalli, MT Swinhoe, CD Rael. 2011. State Of The Art Monte Carlo Modeling Of Active Collar Measurements And Comparison With Experiment. Los Alamos National Laboratory. INMM Conference Record 2011.
- Canberra. 2011. Model JCC-71, 72 and 73 Neutron Coincidence Collars. Accessed at www.canberra.com.
- Harker W, W Hansen, M Krick, M Smith. 2001. Demonstration Neutron Multiplicity Counter Coincidence Counting Software for Authentication. Technical Report LA-UR-01-4186, Los Alamos National Laboratory.
- Kouzes RT, JH Ely, LE Erikson, WJ Kernan, AT Lintereur, ER Siciliano, DL Stephens, DC Stromswold, RM Van Ginhoven, and ML Woodring. 2010. Neutron detection alternatives for ^3He homeland security.” Nuclear Instruments and Methods in Physics Research A, 623(3):1035-1045.
- Kouzes RT, JH Ely, AT Lintereur, and ER Siciliano. 2012a. Introduction to Neutron Coincidence Counter Design Based on Boron-10. Technical Report PNNL-21090. Pacific Northwest National Laboratory, Richland, WA.
- Kouzes RT, JH Ely, AT Lintereur, and ER Siciliano. 2012b. Boron-10 ABUNCL Prototype Initial Testing. Technical Report PNNL-22147. Pacific Northwest National Laboratory, Richland, WA.
- Lintereur AT, ER Siciliano, and RT Kouzes. 2012. Boron-10 Lined Proportional Counter Model Validation. Technical Report PNNL-21501. Pacific Northwest National Laboratory, Richland, WA.
- PANDA. 1991. Passive Nondestructive Assay of Nuclear Materials (PANDA), Nuclear Regulatory Commission NRC-FIN-A7241. Los Alamos National Laboratory Report LA-UR-90-732. Available at <http://www.lanl.gov/orgs/n/n1/panda/index.shtml>.
- Pelowitz DB (ed.). 2011. “MCNPX User’s Manual”, Version 2.7.0. Los Alamos National Laboratory Report LA-CP-11-00438.
- McKinny, K, T Anderson, N Johnson, E Weissman. 2012. Presentation at the IEEE Nuclear Science Symposium, Anaheim. CA, October 29, 2012.
- Menlove HO. 1981. Description and Performance Characteristics for the Neutron Coincidence Collar for the Verification of Reactor Fuel Assemblies, Los Alamos National Laboratory Report LA-8939-MS.
- Menlove HO, JE Stewart, SZ Qiao, TR Wenz, PD Verrecchia. 1990. Neutron Collar Calibration and Evaluation for Assay of L WR Fuel Assemblies Containing Burnable Neutron Absorbers, Los Alamos National Laboratory Report LA-11965-MS.
- Menlove HO, D Henzlova, LG Evans, MT Swinhoe, and JB Marlow. 2011. ^3He Replacement for Nuclear Safeguards Applications – an Integrated Test Program to Compare Alternative Neutron Detectors. ESARDA Bulletin 46.

Rogers JL, JH Ely, RT Kouzes, AT Lintereur, and ER Siciliano. 2012a. Neutron Coincidence Counting Studies. Technical Report PNNL-21686. Pacific Northwest National Laboratory, Richland, WA.

Rogers JL, JH Ely, RT Kouzes, AT Lintereur, and ER Siciliano. 2012b. Uranium Neutron Coincidence Collar Model Utilizing Boron-10 Lined Tubes. Technical Report PNNL-21750. Pacific Northwest National Laboratory, Richland, WA.

Siciliano ER, and RT Kouzes. 2012a. Boron-10 Lined Proportional Counter Wall Effects. Technical Report PNNL-21368. Pacific Northwest National Laboratory, Richland, WA.

Siciliano ER, JL Rogers, JE Schweppe, AT Lintereur, and RT Kouzes. 2012b. Uranium Neutron Coincidence Collar Model Utilizing ^3He . Technical Report PNNL-21581. Pacific Northwest National Laboratory, Richland, WA.



Pacific Northwest
NATIONAL LABORATORY

902 Battelle Boulevard
P.O. Box 999
Richland, WA 99352
1-888-375-PNNL (7665)

www.pnl.gov



U.S. DEPARTMENT OF
ENERGY